Diamond & Related Materials 131 (2023) 109568

Contents lists available at ScienceDirect

Diamond & Related Materials

journal homepage: www.elsevier.com/locate/diamond

Hydrodynamic thermal transport in BNC_2

Harish PVV, Ankit Jain *

Mechanical Engineering Department, IIT Bombay, India

ARTICLE INFO

Keywords:
Hydrodynamic
Phonon
Thermal transport
Boltzmann transport eq.

ABSTRACT

The thermal transport properties of the recently synthesized high-pressure phase of BNC_2 are investigated using the iterative solution of the Boltzmann transport equation with inputs from density functional theory calculations. The thermal conductivity of BNC_2 is found to be extremely sensitive to pressure and the thermal conductivity at room temperature under 20 GPa pressure is over 1400 W/m-K which is more than 40 % higher than the corresponding value at 0 GPa. Similar to diamond, the origin of this extremely high thermal conductivity is rooted at large phonon group velocities, which gives rise to fluid-like hydrodynamic thermal transport in BNC_2. However, unlike diamond, the large isotope disorder of boron atoms in BNC_2 results in a large phonon-isotope scattering which renders hydrodynamic flow prevalent only in isotopically pure samples at length scales of up to 65 μm at 100 K.

1. Introduction

With continuous reduction in device size and increase in power density, the thermal management is becoming increasingly critical in applications such as microprocessors [1], LEDs [2], and sensors [3]. Identifying new materials with high thermal conductivity is, thus, becoming inevitable. Conventionally, the high material thermal conductivities are observed in carbon based materials, diamond and graphite, with room temperature thermal conductivities of 2200 W/m-K and 1910 W/m-K respectively [4–6]. Recently, thermal transport properties of BNC_2 are investigated by Wu et al. [7] using the density functional theory (DFT) driven solution of the Boltzmann transport equation (BTE) and high thermal conductivity of 1242 W/m-K was obtained. The origin of this high thermal conductivity is found to be large acoustic phonon group velocities, as is the case for carbon-based materials [5,8]. The authors, however, limited their study to ambient pressure, though the studied phases of BNC_2 are stable only at high pressures [9–12]. Previous literature studies have shown that the pressure-dependence of thermal conductivity is a result of interplay of harmonic and anharmonic lattice properties and the thermal conductivity could increase or decrease with pressure depending on the material system [13,14]. As such, there is a need to study the effect of pressure on the thermal transport properties of BNC_2.

Furthermore, for materials with large phonon group velocities, the majority of the active phonons at room temperature and below are close of the zone center of the Brillouin zone. Under such circumstances, the dominant intrinsic scattering of phonons is via momentum conserving Normal ($\mathcal{N}$) phonon-phonon scattering processes [as opposed to momentum destroying Umklapp ($\mathcal{U}$) processes in other materials] and the corresponding phonon flow is hydrodynamic-like, resembling similarities with the drifted macroscopic motion of fluid particles [15]. For the majority of materials, the phonon flow is ballistic at low temperatures and transforms to diffusive at high temperatures with no or a very small temperature window near the peak of thermal conductivity at cryogenic temperatures for hydrodynamic flow [15]. Consequently, the hydrodynamic flow is observed experimentally only in a handful of exotic materials: (1) ^{3}He at temperatures between 0.42 and 0.58 K [16], (2) Bi between 1.2 and 4 K [17], (3) NaF between 11 and 14.5 K [18,19], and more recently for (4) graphene between 85 and 125 K [15]. Computationally, the hydrodynamic flow is also suggested to exist in few other two-dimensional materials and in diamond [20]. Because of a similar origin of high thermal conductivity in BNC_2 as that in diamond, there is a possibility of hydrodynamic flow of phonons in BNC_2, not yet explored.

In this work, using first-principles calculations, we explored (a) the effect of pressure on thermal transport properties and (b) the possibility of hydrodynamic thermal transport in orthorhombic-phase of BNC_2 which is reported to be experimentally stable at pressures between 10 and 30 GPa [10–12]. We find that the thermal conductivity of BNC_2 increases with pressure and the predicted thermal conductivity at room temperature at 20 GPa is 43 % higher than that at ambient pressure. Further, we find that phonon flow is hydrodynamic-like in isotopically

* Corresponding author.
E-mail address: a_jain@iitb.ac.in (A. Jain).

https://doi.org/10.1016/j.diamond.2022.109568
Received 16 September 2022; Accepted 20 November 2022
Available online 25 November 2022

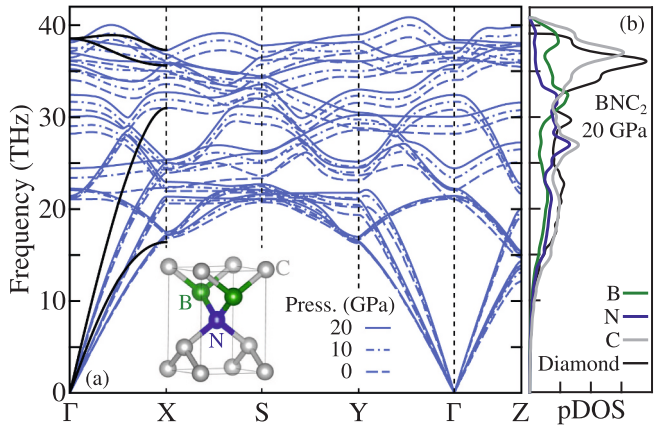

Fig. 1. (a) The effect of pressure on phonon dispersion of BNC_2. The phonon dispersion of diamond (at 0 GPa) is also included in the Γ-X direction for comparison. (b) The atom-decomposed phonon density of states for BNC_2 at 20 GPa.

pure BNC_2 at temperatures below 100 K with the characteristic second sound propagation length of 64 μm (compared to 7 μm and 409 μm in naturally-occurring and isotopically enriched diamond) at 100 K.

2. Computational details

The crystal structure of orthorhombic phase of BNC_2 with space group *Pmm*2 is presented in inset of Fig. 1. The crystal structure resembles that of diamond, where each carbon atom is tetrahedrally bonded to two carbon atoms, a boron atom, and a nitrogen atom. As this BNC_2 phase is reported to be stable at 10–30 GPa, the phonon transport calculations are carried out at 0, 10, and 20 GPa using full iterative solution of the BTE as [21,22]:

$$k_\alpha = \sum_i c_{ph,i} v_{\alpha,i}^2 \tau_i. \tag{1}$$

The summation in Eq. (1) is over all the phonon modes in the Brillouin zone and c_{ph}, ν_α, and τ are the phonon specific heat, group velocity (α-component), and scattering lifetime, respectively. The details regarding c_{ph}, ν_α, and τ calculations are available elsewhere in Refs [22–24].

The structure relaxation and force constant calculations were carried out using Quantum Espresso package with norm conserving pseudopotentials with converged electronic wavevector grid and plane wave energy cutoff of 6 × 6 × 6 and 80 Ry respectively [25,26]. The harmonic force constants are initially obtained on a 6 × 6 × 6 phonon wavevector grid using density functional perturbation theory [27] and are later interpolated to 22 × 22 × 22 grid for lattice thermal conductivity calculations. The anharmonic force constants are obtained using the stochastic thermal snapshot technique [28–30] using 200 thermally populated supercells of 256 atoms each corresponding to a temperature of 300 K. The cubic interaction cutoff is fixed at 4 Å for the extraction of anharmonic force constants from the force-displacement data fitting. Since the high thermal conductivity of BNC_2 originates from high group velocity of phonons (and not due to suppression of three-phonon scattering originating from reduced scattering phase-space), we considered only three-phonon scattering processes in the evaluation of phonon scattering rates.

The presence of hydrodynamic flow is explored through second-sound length and averaged linewidths of $\mathscr{N}$, $\mathscr{U}$, and $\mathscr{I}$ processes. The characteristic second sound propagation length scale is obtained as $\lambda = \nu_{ss}\tau_{ss}$, where ν_{ss} and τ_{ss} are velocity and timescale for second sound, given by [15]

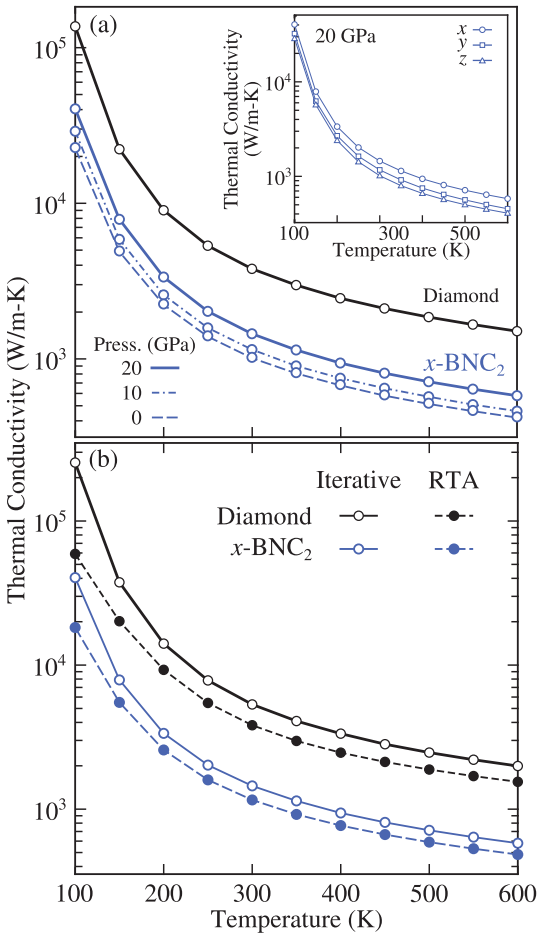

Fig. 2. (a) The effect of pressure on the *x*-direction thermal conductivity of BNC_2 as obtained by the full/iterative solution of the Boltzmann transport equation (BTE) and (b) the effect of iterative/full solution of the BTE on the predicted *x*-direction thermal conductivity as compared to the relaxation time approximation (RTA). The direction-dependent thermal conductivities of BNC_2 are reported in the inset of (a) for 20 GPa. The thermal conductivity values for diamond are also included in (a) and (b) for comparison. All reported conductivities are for isotopically pure samples.

$$v_{ss}^2 = \frac{\sum_i^1 c_{ph,i} v^2}{\sum_i c_{ph,i}}, \tag{2}$$

$$\frac{1}{\tau_{ss}} = \frac{\sum_i n_i(n_i+1)\hbar\omega_i v_i^\alpha q^\alpha \Big/ \tau_i^R}{\sum_i n_i(n_i+1)\hbar\omega_i v_i^\alpha q^\alpha}, \tag{3}$$

and the averaged linewidths are obtained as

$$\Gamma^p = \frac{\sum_i c_{ph} 2\pi \Big/ \tau_i^p}{\sum_i c_{ph}}, \tag{4}$$

with n_i, ω_i, $\mathbf{q}$, and τ_i^R representing phonon equilibrium population, frequency, wavevector, and resistive scattering lifetime and p denotes the type of scattering process.

3. Results

We start by first investigating the effect of pressure on phonon frequencies of orthorhombic phase of BNC_2 in Fig. 1. The desired pressures

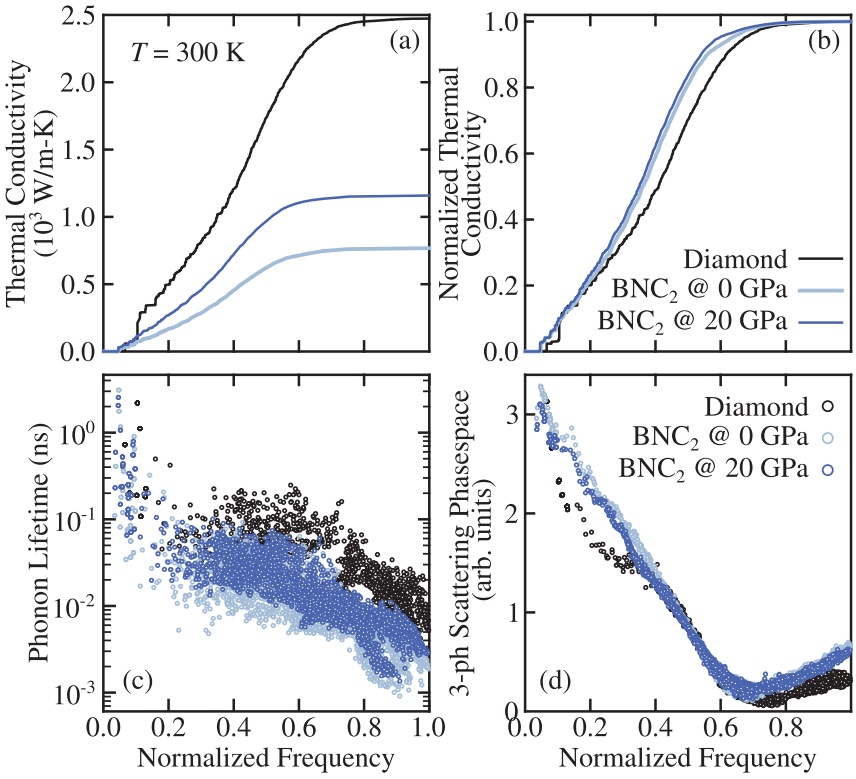

Fig. 3. (a) The thermal conductivity accumulation, (b) normalized thermal conductivity accumulation, (c) three-phonon scattering lifetime, and (d) three-phonon scattering phase space plotted against normalized phonon frequency for BNC_2 at 0 and 20 GPa. The phonon frequencies at a given pressure are normalized by the maximum phonon frequency at that pressure. All results are for isotopically pure samples at a temperature of 300 K.

of 10 and 20 GPa are obtained by isotropic compression of relaxed structure by 0.82 % and 1.55 % respectively. For comparison, we also plotted phonon dispersion of diamond at zero pressure in the $\Gamma - X$ direction in Fig. 1.

Overall, we find that the range of phonon frequencies in BNC_2 is similar to that in diamond. Both materials are stiff and have sound velocities (longitudinal acoustic phonon group velocity in the $\Gamma - X$ direction in the large wavevector limit) of 17.6 and 18.2 km/s. These sound velocities are a factor of 2–3 higher than other compounds (for instance, 6–7 km/s in silicon [31]) and are reported as the reason for high thermal conductivity in carbon based systems [5] (note that the abscissa in Fig. 1 are normalized by the lattice constant and the slope of dispersion branches, as such, does not reflect the absolute phonon group velocities). Furthermore, like in diamond, all involved species have similar mass in BNC_2, resulting in delocalized modes as is evident from similar partial density of states of each of participating atoms. In comparison with diamond, the unitcell of BNC_2 is more complex and has more dispersion branches. This complex unitcell of BNC_2 opens up more possibilities for satisfying three-phonon scattering selection rules and results in an enhanced three-phonon scattering phase space of low-frequency phonons as compared to that in diamond as is shown later in Fig. 3(d). Further, the orthorhombic structure of BNC_2 results in anisotropic dispersion with sound velocities of 17.6, 16.7, and 16.9 km/s in three orthonormal directions. With increasing pressure, the phonon frequencies, and hence group velocities, increase all across the Brillouin zone for BNC_2. This increase in phonon frequencies originates from stiffening of bonds (as is reported in literature for silicon [13]) and is similar in three perpendicular directions for BNC_2.

The temperature-dependence of directional thermal conductivities of BNC_2 at 20 GPa is reported in the inset of Fig. 2(a). The thermal conductivity follows the same trend as that of group velocity and is highest in the x-direction followed by y- and z-directions. For the temperature range considered, the thermal transport anisotropy is highest at 600 K and the anisotropy decreases with reducing temperature to 1.45 at 100 K. At a temperature of 300 K, the x-direction thermal conductivity of isotopically pure BNC_2 is 1012 W/m-K compared to 3791 W/m-K for diamond under similar conditions [Fig. 2(a)]. This is despite the larger anharmonicity of diamond as is reflected in a larger heat capacity weighted average Grüneisen parameter value of 0.76 in diamond compared to 0.71 in BNC_2 at 0 GPa; thereby suggesting that the four times higher thermal conductivity of diamond is predominantly a result of large phonon group velocities and reduced three-phonon scattering phase space.

With pressure, the thermal conductivity increases for all directions and the x-direction thermal conductivity increases by 43 % at 20 GPa compared to its value at 0 GPa. The corresponding change in phonon properties with pressure is presented in Fig. 3. We find that at both, 0 and 20 GPa, the thermal transport is dominated by phonons with frequencies up to 25 THz. In going from 0 to 20 GPa, as mentioned earlier, while the group velocities increase due to stiffening of phonons, the increase in heat-capacity weighted group velocity square ($\sum_i c_{v,i} v_{g}^2 / \sum_i c_{v,i}$) is only ~9.7 %, insufficient to explain the 43 % increase of the thermal conductivity. As shown in Fig. 3(c), however, with increasing pressure, the phonon lifetimes also more than double for most of the heat carrying phonon modes. This increase in phonon lifetimes along with accompanying increasing in group velocities is responsible for the predicted increase of thermal conductivity with pressure. It is worthwhile to mention that the phonon modes in BNC_2 are more anharmonic at higher pressure. The heat-capacity weighted Grüneisen parameter at 20 GPa is 0.76 compared to 0.72 as 0 GPa. Despite this increase in anharmonicity, the phonon lifetimes increase at higher pressure due to a reduction in the three-phonon scattering phase space [see Fig. 3(d)].

The thermal conductivities reported in Fig. 2(a) are obtained using the iterative/full solution of the BTE. Using the RTA solution, the thermal conductivities are under-predicted by a factor of 1.3 in BNC_2 in the x-direction at 300 K at 0 GPa. The corresponding under-prediction in

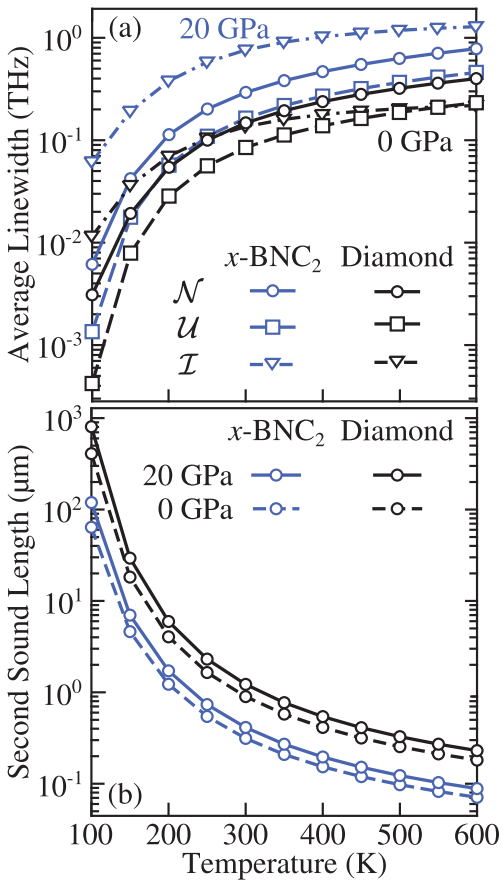

Fig. 4. (a) The temperature-dependent average phonon linewidths for Normal, Umklapp, and isotope scattering processes in diamond (0 GPa) and BNC_2 (20 GPa). (b) The temperature-dependence of characteristic second-sound length in isotopically pure BNC_2 and its comparison with diamond.

diamond is by a factor of 1.5. This under-prediction of thermal conductivity by RTA solution is due to a large fraction of momentum-conserving $\mathcal{N}$ three-phonon scattering processes which are wrongly treated as resistive by the RTA solution [32,33]. The fraction of such processes is generally small in other non-carbon based materials where the thermal conductivity changes are less than 5 % with the use of iterative solution of the BTE [6]. The large fraction of $\mathcal{N}$ scattering processes points to a possibility of hydrodynamic transport and second sound at low temperatures [15]. To test for this, we compute the heat capacity weighted average phonon linewidths [15] corresponding to the $\mathcal{N}$, $\mathcal{U}$, and $\mathcal{I}$ phonon scattering and report the results in Fig. 4.

We find that for both, diamond and BNC_2, the phonon-phonon scattering is dominated by $\mathcal{N}$ processes. However, while the isotope scattering is only dominant at low temperatures in diamond, owing to large isotope disorder of boron atoms, the isotope-scattering is the dominant phonon scattering mechanism in the entire considered temperature range in BNC_2. This suggests that, like in diamond, while there is a possibility of hydrodynamic flow in BNC_2, it is possible only in isotopically pure samples. The hydrodynamic flow is also characterized by the presence of second sound, i.e., the observation of two response wave pulses for a given thermal perturbation; first corresponding to relaxation of carriers to drifted Bose-Einstein distribution via momentum conserving $\mathcal{N}$ processes with timescale τ_N and second corresponding to subsequent relaxation of carriers to equilibrium Bose-Einstein distribution via non-momentum conserving $\mathcal{U}$ processes with timescale τ_U [15]. At a temperature of 100 K, the characteristic second-sound length [15] in isotopically pure BNC_2 is 64 μm as compared to 407 μm in diamond, thus suggesting that second-sound exists at smaller length scales in BNC_2 and the measurements need to resolve length scales lower than 64 μm in order to detect second-sound in BNC_2 at 100 K.

4. Conclusions

We employed density functional theory and solved the Boltzmann transport equation to study the effect of pressure on the recently synthesized high-pressure orthorhombic phase of BNC_2. We find that due to light masses of involved atoms and stiff bonds, the phonon group velocities are large in BNC_2, similar to that in diamond. Nevertheless, due to its complex unitcell, the predicted thermal conductivity of isotopically pure BNC_2 is more than a factor of 3 lower that of isotopically pure diamond under ambient conditions. The thermal conductivity of BNC_2 increases with pressure and reaches 1450 W/m-K at 20 GPa. Because of the similar origin of high thermal conductivity in BNC_2 as that in diamond, BNC_2 also has significant momentum conserving $\mathcal{N}$ phonon-phonon scattering, resulting in a hydrodynamic-like phonon flow at low temperatures. However, due to a large isotope disorder of boron atoms, unlike diamond, this hydrodynamic-like flow is observable only in isotopically pure BNC_2 samples with characteristic length scale smaller than 65 μm at 100 K.

Declaration of competing interest

The authors declare that they have no known competing financial interests or personal relationships that could have appeared to influence the work reported in this paper.

Data availability

The raw/processed data required to reproduce these findings is available on a reasonable request via email.

Acknowledgement

The authors acknowledge the financial support from IRCC-IIT Bombay and National Supercomputing Mission, Government of India (Grant Number: DST/NSM/R&D-HPC-Applications/2021/10). The calculations are carried out on SpaceTime-II supercomputing facility of IIT Bombay and PARAM Sanganak supercomputing facility of IIT Kanpur.

References

[1] F. Sarvar, D. Whalley, P. Conway, 2006 1st Electronic Systemintegration Technology Conference, IEEE, 2006.
[2] M. Arik, C.A. Becker, S.E. Weaver, J. Petroski, in: I.T. Ferguson, N. Narendran, S. P. DenBaars, J.C. Carrano (Eds.), SPIE Proceedings, SPIE, 2004.
[3] Y. Zeng, T. Li, Y. Yao, T. Li, L. Hu, A. Marconnet, Adv. Funct. Mater. 1901388 (2019).
[4] P. Klemens, D. Pedraza, Carbon 32 (1994) 735.
[5] A. Ward, D.A. Broido, D.A. Stewart, G. Deinzer, Phys. Rev. B 80 (2009), 125203.
[6] L. Lindsay, D.A. Broido, T.L. Reinecke, Phys. Rev. B 87 (2013), 165201.
[7] H. Wu, H. Fan, Y. Hu, Phys. Rev. B 103 (2021) 41203.
[8] L. Lindsay, D.A. Broido, T.L. Reinecke, Phys. Rev. B 87 (2013), 165201.
[9] E. Knittle', R.B. Kaner, R. Jeanloz, M.L. Cohen, NUMBER, Tech. Rep, 1995.
[10] M. Mattesini, S. Matar, Int. J. Inorg. Mater. 3 (2001) 943.
[11] V.L. Solozhenko, D. Andrault, G. Fiquet, M. Mezouar, D.C. Rubie, Appl. Phys. Lett. 78 (2001) 1385.
[12] Y. Zhao, D.W. He, L.L. Daemen, T.D. Shen, R.B. Schwarz, Y. Zhu, D.L. Bish, J. Huang, J. Zhang, G. Shen, J. Qian, T.W. Zerda, J. Mater. Res. 17 (2002) 3139.
[13] K.D. Parrish, A. Jain, J.M. Larkin, W.A. Saidi, A.J.H. McGaughey, Phys. Rev. B 90 (2014), 235201.
[14] D.A. Broido, L. Lindsay, A. Ward, Phys. Rev. B 86 (2012), https://doi.org/10.1103/phys-revb.86.115203.
[15] A. Cepellotti, G. Fugallo, L. Paulatto, M. Lazzeri, F. Mauri, N. Marzari, Nat. Commun. 6 (2015) 1.
[16] C.C. Ackerman, W.C. Overton, Phys. Rev. Lett. 22 (1969) 764.
[17] V. Narayanamurti, R.C. Dynes, Phys. Rev. Lett. 28 (1972) 1461.
[18] H.E. Jackson, C.T. Walker, T.F. McNelly, Phys. Rev. Lett. 25 (1970) 26.
[19] T.F. McNelly, S.J. Rogers, D.J. Channin, R.J. Rollefson, W.M. Goubau, G. E. Schmidt, J.A. Krumhansl, R.O. Pohl, Phys. Rev. Lett. 24 (1970) 100.

[20] S. Lee, D. Broido, K. Esfarjani, G. Chen, Nat. Commun. 6 (2015) 1.
[21] J.M. Ziman, Electrons and Phonons, Oxford University Press, Clarendon, Oxford, 1960.
[22] J.A. Reissland, The Physics of Phonons, John Wiley and Sons Ltd, 1973.
[23] A.J. McGaughey, A. Jain, H.-Y. Kim, B. Fu, J. Appl. Phys. 125 (2019), 011101.
[24] A. Jain, Phys. Rev. B 102 (2020), https://doi.org/10.1103/physrevb.102.201201.
[25] P. Giannozzi, S. Baroni, N. Bonini, M. Calandra, R. Car, C. Cavazzoni, D. Ceresoli, G.L. Chiarotti, M. Cococcioni, I. Dabo, A.D. Corso, S. de Gironcoli, S. Fabris, G. Fratesi, R. Gebauer, U. Gerstmann, C. Gougoussis, A. Kokalj, M. Lazzeri, L. Martin-Samos, N. Marzari, F. Mauri, R. Mazzarello, S. Paolini, A. Pasquarello, L. Paulatto, C. Sbraccia, S. Scandolo, G. Sclauzero, A.P. Seitsonen, A. Smogunov, P. Umari, R.M. Wentzcovitch, J. Phys.-Condens. Mater. 21 (2009), 395502.
[26] D.R. Hamann, Phys. Rev. B 88 (2013), 085117.
[27] S. Baroni, S. de Gironcoli, A. Dal Corso, P. Giannozzi, Rev. Mod. Phys. 73 (2001) 515.
[28] D. West, S. Estreicher, Phys. Rev. Lett. 96 (2006), 115504.
[29] O. Hellman, P. Steneteg, I.A. Abrikosov, S.I. Simak, Phys. Rev. B 87 (2013), 104111.
[30] N. Shulumba, O. Hellman, A.J. Minnich, Phys. Rev. B 95 (2017), 014302.
[31] A. Jain, A.J. McGaughey, Comput. Mater. Sci. 110 (2015) 115.
[32] M. Omini, A. Sparavigna, Nuovo Cimento D 19 (1997) 1537.
[33] D.A. Broido, A. Ward, N. Mingo, Phys. Rev. B 72 (2005), 014308.